NIST Internal Report
NIST IR 8474

An Equation of State for the Thermodynamic Properties of Helium

Diego O. Ortiz Vega
Kenneth R. Hall
James C. Holste
Allan H. Harvey
Eric W. Lemmon

This publication is available free of charge from:
https://doi.org/10.6028/NIST.IR.8474

NIST NATIONAL INSTITUTE OF STANDARDS AND TECHNOLOGY
U.S. DEPARTMENT OF COMMERCE

NIST Internal Report
NIST IR 8474

An Equation of State for the Thermodynamic Properties of Helium

Diego O. Ortiz Vega
Kenneth R. Hall
James C. Holste
Department of Chemical Engineering
Texas A&M University

Allan H. Harvey
Eric W. Lemmon
Applied Chemicals and Materials Division
Material Measurement Laboratory
National Institute of Standards and Technology

This publication is available free of charge from:
https://doi.org/10.6028/NIST.IR.8474

August 2023

U.S. Department of Commerce
Gina M. Raimondo, Secretary

National Institute of Standards and Technology
Laurie E. Locascio, NIST Director and Under Secretary of Commerce for Standards and Technology

NIST IR 8474
August 2023

Certain commercial equipment, instruments, software, or materials, commercial or non-commercial, are identified in this paper in order to specify the experimental procedure adequately. Such identification does not imply recommendation or endorsement of any product or service by NIST, nor does it imply that the materials or equipment identified are necessarily the best available for the purpose.

Publication History
Approved by the NIST Editorial Review Board on 2023-07-07

How to Cite this NIST Technical Series Publication
Ortiz Vega DO, Hall KR, Holste JC, Harvey AH, Lemmon EW (2023) An Equation of State for the Thermodynamic Properties of Helium. (National Institute of Standards and Technology, Gaithersburg, MD), NIST Internal Report (IR) NIST IR 8474. https://doi.org/10.6028/NIST.IR.8474

NIST Author ORCID iDs
Allan H. Harvey: 0000-0003-0073-2332
Eric W. Lemmon: 0000-0002-0974-0203

Contact Information
allan.harvey@nist.gov

Abstract

This report documents the equation of state for fluid helium implemented in Version 10 of NIST's REFPROP Standard Reference Database. The equation of state is expressed as the molar Helmholtz energy as a function of temperature and density, and is valid for the normal fluid (helium I) up to 1500 K and 2000 MPa. Limited comparisons with experimental data and with virial coefficients calculated by *ab initio* methods are provided.

Keywords

equation of state; helium; thermodynamic properties; virial coefficients.

Table of Contents

List of Tables

List of Figures

1. Background of this Report

In the early 2010s, NIST and Texas A&M University undertook a joint effort to develop a new reference equation of state for helium. An equation of state was presented in the 2013 thesis of Ortiz Vega [1]. That equation was incorporated in Version 9.1 and (after some modifications) in Version 10 of NIST's REFPROP database [2].

At that time, it was planned to document the final equation of state in an article in an archival journal. However, several years ago it was recognized that there was still significant room for improvement in the equation of state. In particular, insufficient attention had been paid to the nuances of cryogenic temperature scales; some conversions to the International Temperature Scale of 1990 (ITS-90) [3, 4] were not performed correctly and the equation of state did not satisfy the relationship between temperature and vapor pressure that forms part of the definition of ITS-90. In addition, some cryogenic density data that were taken with a dielectric method had not been corrected for improved knowledge of the dielectric polarizability of helium [5] that should supersede the 1950s values used in the original experimental papers.

For these reasons, NIST intends to produce a new, comprehensive reference equation of state for helium. However, this is still some distance in the future due to other priorities. In the meantime, we provide this brief report in order to supply archival documentation for the preliminary equation of state that is implemented in REFPROP Version 10.

2. Introduction

Helium is a widely used fluid in science and industry. It is used for cryogenic refrigeration, including in medical applications such as Magnetic Resonance Imaging (MRI) machines and in scientific applications such as particle accelerators. It is used for pressurizing other cryogens (such as liquid hydrogen and oxygen in rockets), as a lifting agent, and in situations where an inert gas is needed. It is also a significant component of some natural gases; the worldwide supply of helium comes from processing these gases.

Scientifically, the unique properties of helium (high thermal conductivity, low condensation temperature, nearness to ideal-gas behavior) lead to its use in many contexts. The ability to calculate from first principles the small deviations of helium properties from that of an ideal gas (due to its small number of electrons) has led to major advances in temperature and pressure metrology based on precise acoustical, electrical, or optical measurements on helium and other noble gases [6].

Helium exists as two stable isotopes: ^{3}He, which contains one neutron, and ^{4}He with two neutrons. The low-temperature behavior of ^{3}He differs greatly from that of ^{4}He because ^{3}He obeys Fermi-Dirac quantum statistics as opposed to the Bose-Einstein statistics of ^{4}He. While ^{3}He has some cryogenic applications, including in the definition of the ITS-90 temperature scale below 3.2 K [3], it is almost nonexistent in natural helium. Our equation of state is therefore developed for ^{4}He. We restrict the equation of state to the normal fluid (helium I), excluding the superfluid (helium II) that forms in liquid ^{4}He below roughly 2 K.

The previous reference equation of state for helium was published by McCarty and Arp in 1990 [7]. While it was useful for its time, it has a variety of shortcomings, as documented by Ortiz Vega [1]. The most significant of these include the relatively limited set of experimental data

used, the failure to fit many data within their experimental uncertainties, and the construction of the equation of state in pressure-explicit form that requires an inconvenient integration and supplementation by a separate heat-capacity formulation to obtain caloric properties.

In this work, we use the state-of-the-art approach for equation-of-state development. The equation is constructed as a single thermodynamic potential, giving the Helmholtz energy as a function of temperature and density. All thermodynamic properties can then be obtained by appropriate mathematical operations on the Helmholtz energy function.

3. Physical Constants and Characteristic Properties

The equation of state makes use of fundamental constants, such as the molar gas constant R, and also the state parameters of the fluid at the critical point. These values are given in Table 1. The critical parameters were obtained as part of the optimization process, starting with the values recommended by McCarty and Arp [7]. The molar mass M is needed to convert between mass-based and mole-based properties. We note that the value of R used differs slightly from the latest CODATA recommendation [8]; the value in Table 1 should be used in implementing the equation of state because it corresponds to the value used in fitting the equation.

Table 1. Physical constants and characteristic properties of helium.

Symbol	Quantity	Value
R	Molar gas constant	8.314472 J·mol^{-1}·K^{-1}
M	Molar mass	4.002602 g·mol^{-1}
T_c	Critical temperature	5.1953 K
p_c	Critical pressure	0.22832 MPa
ρ_c	Critical density	17.3837 mol·dm^{-3}
T_{nbp}	Normal boiling point temperature	4.2238 K

4. The Equation of State

The equation of state is written as the sum of an ideal-gas term and a residual term:

$$a(T,\rho) = a^{o}(T,\rho) + a^{r}(T,\rho), \tag{1}$$

where a is the molar Helmholtz energy, T is the absolute temperature, and ρ is the molar density. $a°$ is the Helmholtz energy of the ideal gas, while a^r is the residual term describing contributions to the Helmholtz energy from interactions between helium atoms. The dimensionless Helmholtz energy can be defined by $\alpha = a/RT$, resulting in

$$\alpha(\tau,\delta) = \frac{a(T,\rho)}{RT} = \frac{a^{o}(T,\rho)}{RT} + \frac{a^{r}(T,\rho)}{RT} = \alpha^{o}(\tau,\delta) + \alpha^{r}(\tau,\delta), \tag{2}$$

where the reduced reciprocal temperature is $\tau \equiv T_c/T$ and the reduced density is $\delta \equiv \rho/\rho_c$.

4.1. The Ideal-gas Helmholtz Energy

The Helmholtz energy of an ideal gas can be obtained by integrating the ideal-gas heat capacity c_p° and incorporating constants of integration based on the chosen reference state. For a monatomic gas, c_p° has a constant value of 2.5R, resulting in

$$\alpha^\circ(\delta,\tau) = a_1 + a_2\tau + \ln\delta + 1.5\ln\tau \,. \tag{3}$$

The constants a_1 and a_2 are adjusted so that the enthalpy and entropy agree with the (arbitrary) reference state chosen for the equation of state. In this case, the default reference state in REFPROP is for the enthalpy and entropy of the saturated liquid to be zero at the normal boiling point. This results in a_1 = 0.1733487932835764 and a_2 = 0.4674522201550815.

4.2. The Residual Helmholtz Energy

The residual Helmholtz energy is an empirical expression whose general form has been developed over many years of fitting reference equations of state. It is written as

$$\begin{aligned}\alpha^{\mathrm{r}}(\tau,\delta) &= \alpha^{\mathrm{r}}_{\mathrm{Pol}} + \alpha^{\mathrm{r}}_{\mathrm{Exp}} + \alpha^{\mathrm{r}}_{\mathrm{GBS}} \\ &= \sum_{i=1}^{I_{\mathrm{Pol}}} n_i \delta^{d_i}\tau^{t_i} + \sum_{i=I_{\mathrm{Pol}}+1}^{I_{\mathrm{Pol}}+I_{\mathrm{Exp}}} n_i \delta^{d_i}\tau^{t_i}\exp\left(-\delta^{l_i}\right) + \\ &\quad \sum_{i=I_{\mathrm{Pol}}+I_{\mathrm{Exp}}+1}^{I_{\mathrm{Pol}}+I_{\mathrm{Exp}}+I_{\mathrm{GBS}}} n_i \delta^{d_i}\tau^{t_i}\exp\left[-\eta_i(\delta-\varepsilon_i)^2 - \beta_i(\tau-\gamma_i)^2\right]\end{aligned}, \tag{4}$$

where I_{Pol}, I_{Exp}, and I_{GBS} are the number of polynomial-like terms, exponential terms, and Gaussian bell-shaped terms, respectively. In this work, I_{Pol} = 6, I_{Exp} = 6, and I_{GBS} = 11. The parameters in Eq. (4) are given in Table 2.

Table 2. Parameters and coefficients of the equation of state.

i	n_i	t_i	d_i	l_i	η_i	β_i	γ_i	ε_i
1	0.015559018	1.0	4					
2	3.0638932	0.425	1					
3	–4.2420844	0.63	1					
4	0.054418088	0.69	2					
5	–0.18971904	1.83	2					
6	0.087856262	0.575	3					
7	2.2833566	0.925	1	1				
8	–0.53331595	1.585	1	2				
9	–0.53296502	1.69	3	2				
10	0.99444915	1.51	2	1				
11	–0.30078896	2.9	2	2				
12	–1.6432563	0.8	1	1				
13	0.8029102	1.26	2		1.5497	0.2471	3.15	0.596
14	0.026838669	3.51	1		9.245	0.0983	2.54505	0.3423
15	0.04687678	2.785	2		4.76323	0.1556	1.2513	0.761
16	–0.14832766	1.0	1		6.3826	2.6782	1.9416	0.9747
17	0.03016211	4.22	1		8.7023	2.7077	0.5984	0.5868
18	–0.019986041	0.83	3		0.255	0.6621	2.2282	0.5627
19	0.14283514	1.575	2		0.3523	0.1775	1.606	2.5346
20	0.007418269	3.447	2		0.1492	0.4821	3.815	3.6763
21	–0.22989793	0.73	3		0.05	0.3069	1.61958	4.5245
22	0.79224829	1.634	2		0.1668	0.1758	0.6407	5.039
23	–0.049386338	6.13	2		42.2358	1357.6577	1.076	0.959

5. Results

Because this is only a preliminary equation of state, we will not perform detailed comparisons of calculated properties to data. In the following, we briefly show the performance of the equation of state for a few key properties, making use of selected data sets that we believe to be of relatively high quality.

5.1. Vapor Pressure

The International Temperature Scale of 1990 (ITS-90) uses the vapor pressures of ^{3}He and ^{4}He as part of its definition [3]. Directly relevant to this work, an equation describes the saturated vapor pressure as a function of temperature from the ^{4}He lambda point at 2.1768 K to 5 K. Since our equation of state is on ITS-90, in principle it should give a vapor pressure exactly agreeing with the ITS-90 pressure–temperature relationship, and can be said to be in error by the amount it deviates from that relationship.

Figure 1 plots the relative deviation in vapor pressure from the equation of state compared to the ITS-90 defining relationship between 2.1768 K and 5 K. The equation of state deviates from the ITS-90 definition by amounts on the order of 0.1 % over much of the temperature range. Proper attention to this constraint while fitting a future reference equation of state should be able to reduce this error by at least an order of magnitude.

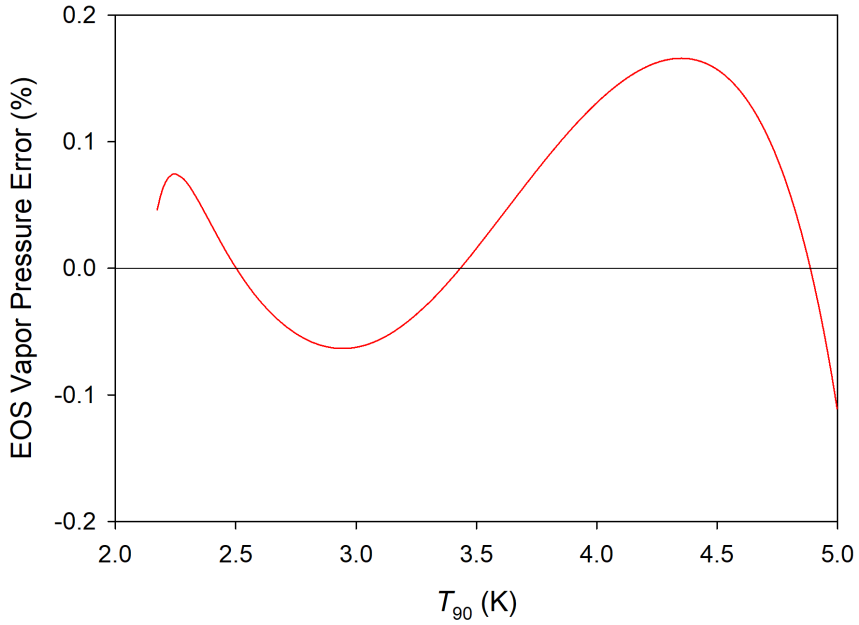

Fig. 1. Relative deviations of vapor pressures calculated with the equation of state from the ^{4}He vapor-pressure relationship used in the definition of ITS-90.

5.2. Virial Coefficients

The virial coefficients describe the deviation of the volumetric behavior of a gas from that of an ideal gas. The second virial coefficient B is the lowest-order deviation (representing a correction that is linear in density), followed by the third virial coefficient C that is multiplied by a term quadratic in density, and so forth.

For helium, *ab initio* quantum chemistry can be used to construct highly accurate intermolecular potentials because each helium atom has only two electrons. The second virial coefficient B can be calculated rigorously from the pair potential, while the calculation of C additionally requires a three-body potential. These calculations provide values with much smaller uncertainties than any existing experiments, so they provide a standard for comparison.

Theoretical values of B from Ref. [9] and of C from Ref. [10] were used to a limited extent in the fitting of our equation of state, although in neither case was the equation forced to agree closely with the values. Both of those studies, however, have been superseded by work that uses potentials of higher accuracy, producing virial coefficients with smaller uncertainties. The best current values of B come from Czachorowski et al. [11], and the best values of C come from Binosi et al. [12].

In Figs. 2 and 3, we compare values of B calculated with our equation of state to the state-of-the art values from Ref. [11]. In Fig. 3, which covers the range from 200–400 K, we also include results from two of the most precise experimental studies [13,14]. While the experimental results agree with the equation of state within their expanded uncertainties, the differences from the theoretical results (which have much smaller expanded uncertainties, near 0.0002 cm^3/mol at the temperatures shown) are many times the uncertainties of those data. The value of B itself is 11–12 cm^3/mol in the range of Fig. 3, so the relative amount by which B from the equation of state is in error at these temperatures is around 0.15 %.

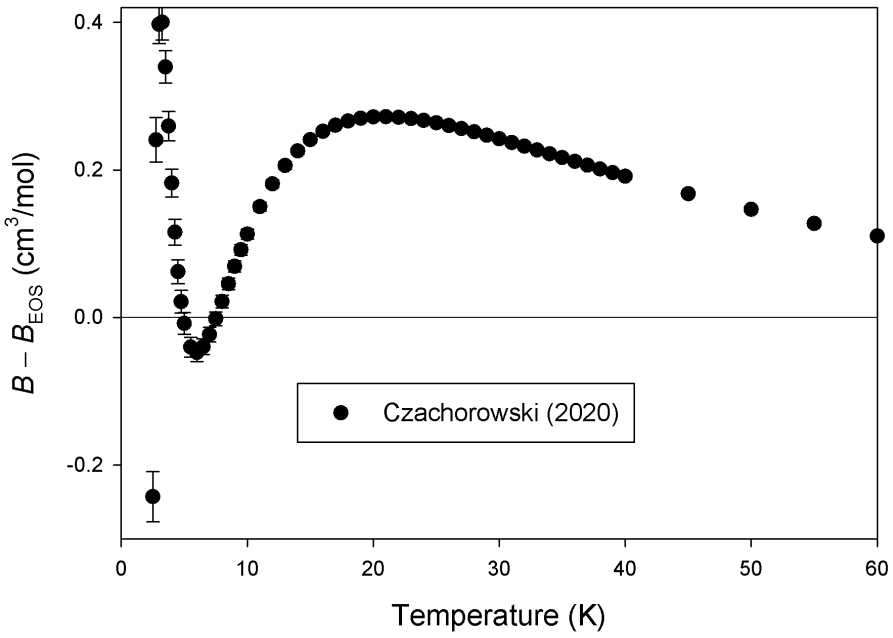

Fig. 2. Differences between highly accurate *ab initio* values of $B(T)$ [11] and those calculated with the equation of state. Error bars represent expanded (k=2) uncertainties and are smaller than the size of the symbols above approximately 10 K.

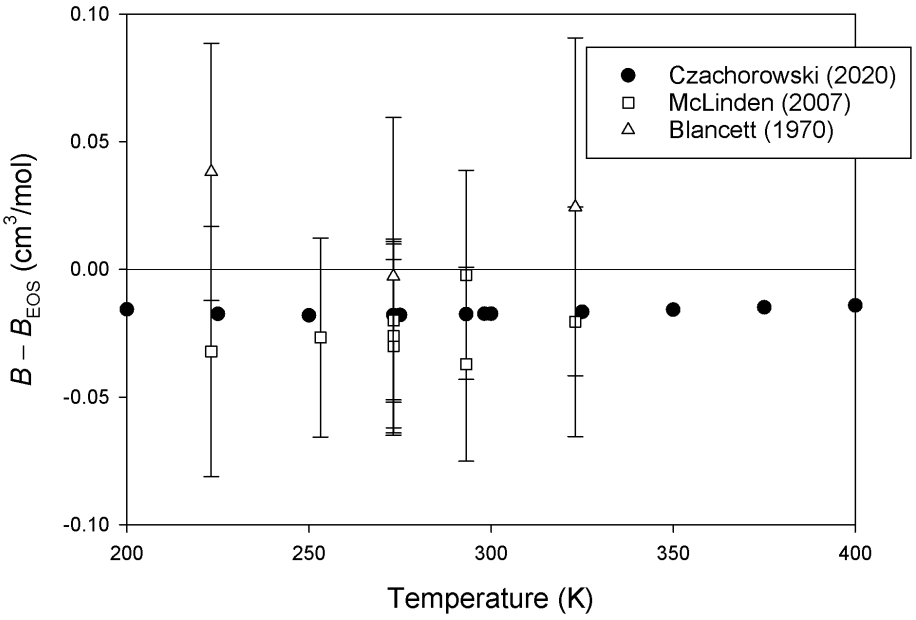

Fig. 3. Differences between highly accurate *ab initio* values of $B(T)$ [11] (and two experimental sources [13,14]) and those calculated with the equation of state. Error bars represent expanded (k=2) uncertainties and are smaller than the size of the symbols for the points from Ref. [11].

Figures 4 and 5 display similar comparisons for C. Similar deviations from the accurate theoretical results are seen, along with agreement with the much more uncertain experimental values. In Fig. 5, the values of C in the range plotted are on the order of 100 cm^6/mol^2, so the corresponding relative errors in C from the equation of state are on the order of 1–2 %.

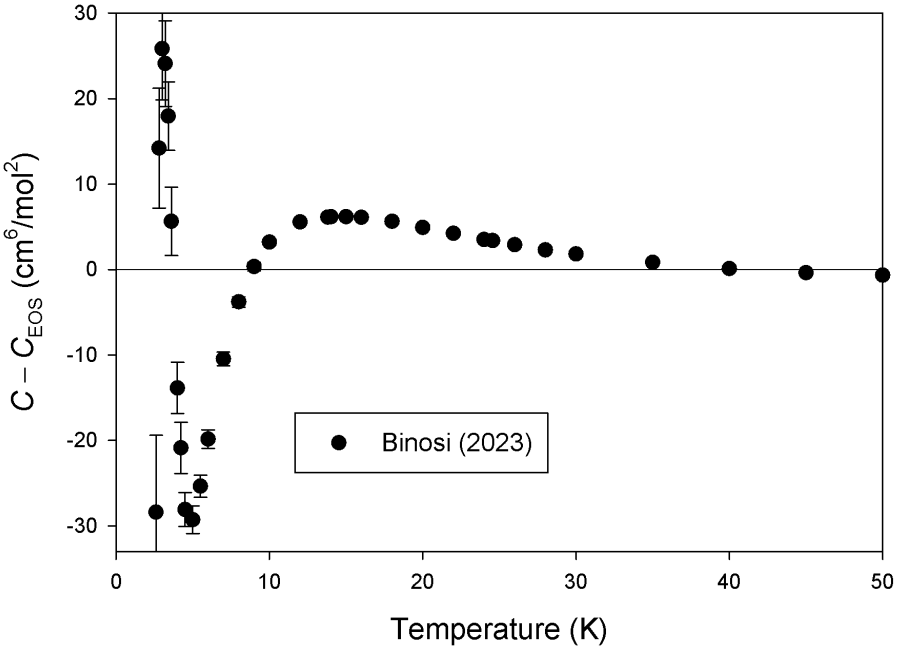

Fig. 4. Differences between highly accurate *ab initio* values of $C(T)$ [12] and those calculated with the equation of state. Error bars represent expanded (k=2) uncertainties and are smaller than the size of the symbols above approximately 8 K.

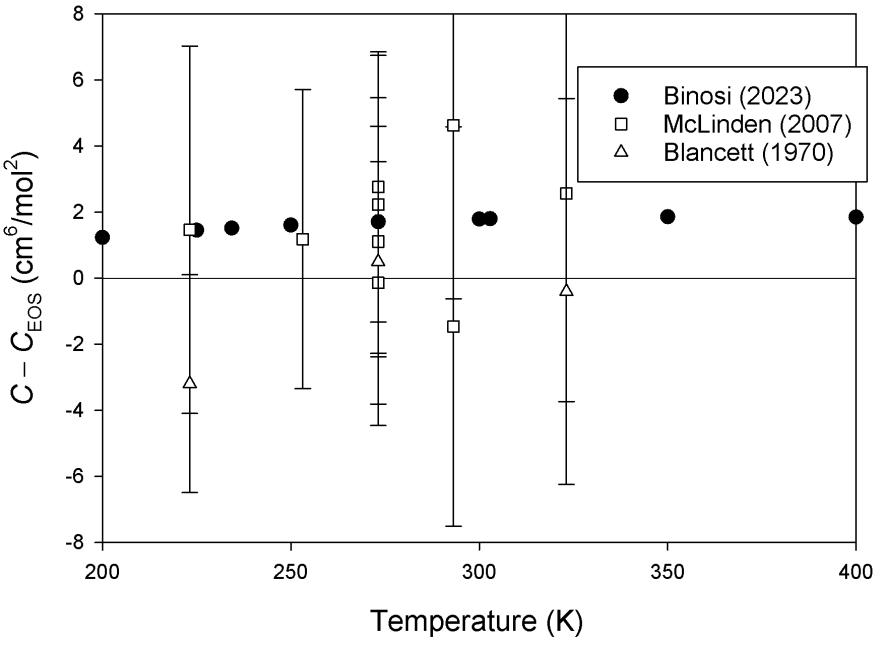

Fig. 5. Differences of highly accurate *ab initio* values of $C(T)$ [12] (and two experimental sources [13,14]) and those calculated with the equation of state. Error bars represent expanded (k=2) uncertainties and are smaller than the size of the symbols for the points from Ref. [12].

For future work, higher virial coefficients have the potential to provide additional constraints for the equation of state. Values of the fourth virial coefficient *D* have been calculated [15,16], but their accuracy is not well defined because no rigorous four-body potential has yet been developed. Higher virial coefficients, up to the seventh, have also been calculated based on accurate two- and three-body potentials [16].

5.3. Density

The density of gaseous helium, especially at temperatures well above its critical temperature, can for the most part be described by the virial expansion for which we have presented comparisons in Sec. 5.2. We therefore limit our comparisons in this region to the high-precision data measured by McLinden and coworkers [13,17] in a two-sinker densimeter between 223 K and 500 K at pressures up to 40 MPa.

We also compare against cryogenic density data, both for liquid helium and for the supercritical fluid at high pressures. We do not attempt exhaustive coverage of the data; instead we choose several studies that appear to be of good accuracy in order to give a general idea of the performance of this preliminary equation of state.

Many reported measurements of helium density at cryogenic temperatures are actually based on measurements of the static dielectric constant that the authors converted to density based on an assumed value for the mean polarizability of helium. There are at least two challenges in using these data. First, the assumed helium polarizability was typically based on older data. The static polarizability of a helium atom can now be calculated from *ab initio* quantum mechanics with very small uncertainty [5]; the state-of-the-art value differs from those previously assumed by relative amounts on the order of 0.2 %. If this were the only issue, the older data could be easily corrected. However, a second problem is that this single-atom polarizability is only rigorously valid in the low-density limit. The first-order correction (second dielectric virial coefficient) has been calculated accurately [18], but it is unclear whether this correction is sufficient, especially at liquid-like densities. The treatment of helium “density” data based on measurements of the dielectric constant (and, closely related, the refractive index) will be discussed in detail in future work. For our present purposes, we will exclude those studies from comparisons with this equation of state.

The liquid density at saturation has been reported by Kerr [19] and by Kerr and Taylor [20]. El Hadi et al. [21] measured the liquid density at pressures slightly above saturation. Grilly and Mills [22] reported liquid densities at high pressures (up to roughly 350 MPa) along the melting curve. The studies of Hill and Lounasmaa [23] and Glassford and Smith [24] both reported densities at liquid and supercritical conditions to high pressures (on the order of 10 MPa for the former and 130 MPa for the latter).

Figures 6 and 7 show the relative deviations from the equation of state for the data of McLinden and Lösch-Will [13] and the data of Moldover and McLinden [17], respectively. While there appear to be some systematic trends in the deviations (which may be due to apparatus factors at the lowest pressures [6]), the deviations are mostly within 0.01 %, which is similar to the uncertainty of the measurements. The good agreement for gas densities is not surprising, since the second and third virial coefficients, *B* and *C*, are fairly accurate as discussed in Sec. 5.2.

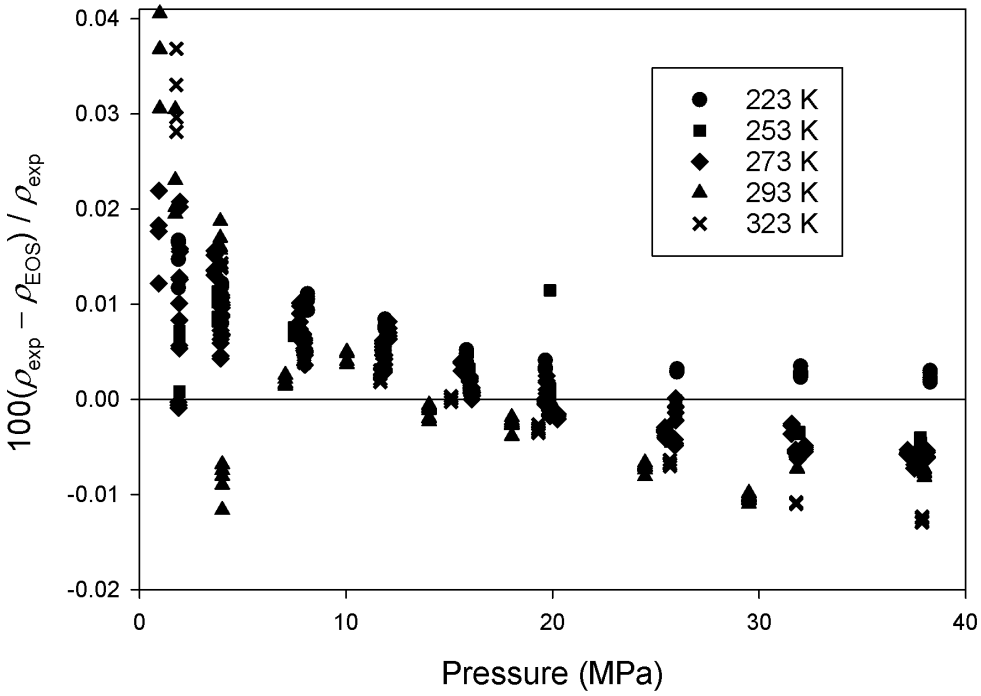

Fig. 6. Relative percent differences between experimental densities from McLinden and Lösch-Will [13] and those calculated with the equation of state.

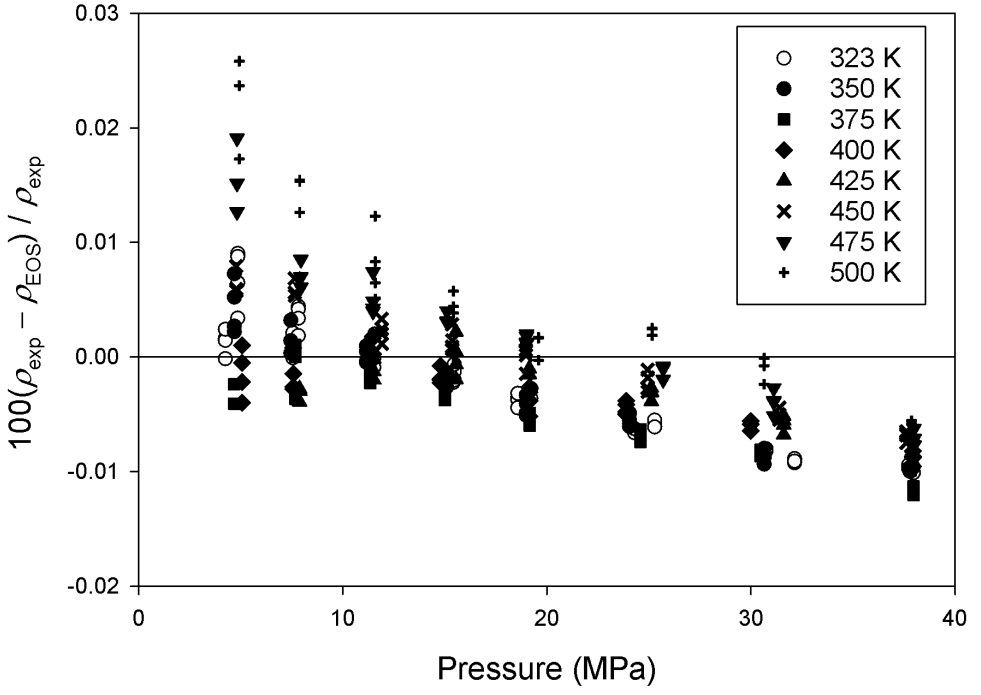

Fig. 7. Relative percent differences between experimental densities from Moldover and McLinden [17] and those calculated with the equation of state.

Figure 8 compares the equation of state to three experimental sources [19-21] for the density of the saturated liquid. The experimental sources are not mutually consistent, but the differences from the equation of state are less than 0.5 % except at the highest temperatures.

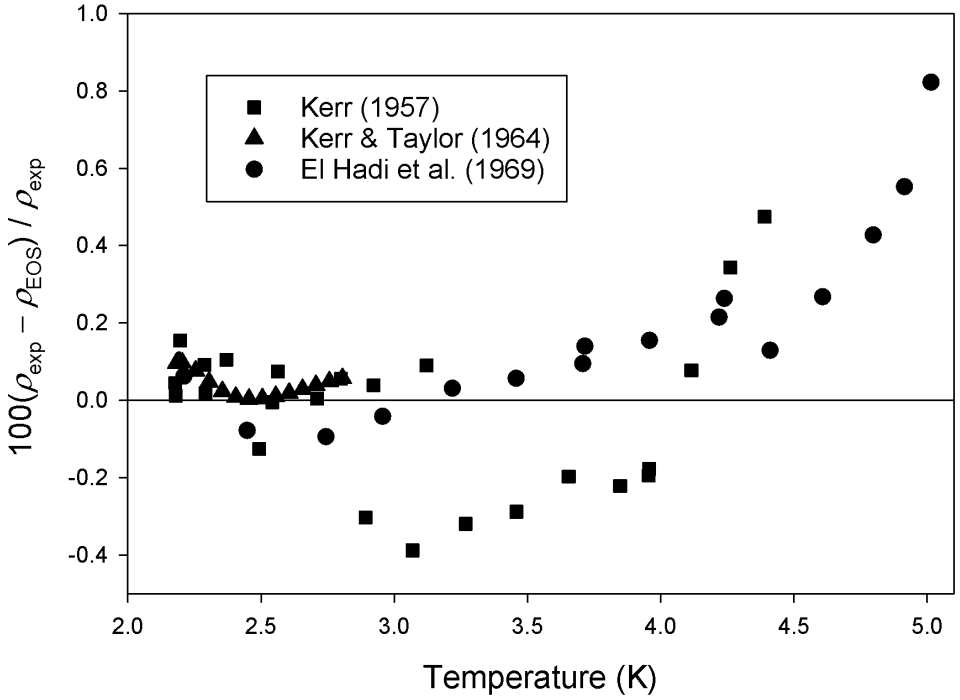

Fig. 8. Relative percent differences between experimental saturated liquid densities [19-21] and those calculated with the equation of state.

Figure 9 shows comparisons to density data for the compressed liquid and supercritical states at cryogenic temperatures (up to approximately 20 K for Hill and Lounasmaa [23] and Glassford and Smith [24]; up to 31 K along the melting curve for Grilly and Mills [22]). Most of the data are represented within 2 %, with larger deviations for a few points from Hill and Lounasmaa that are near the vapor-liquid saturation boundary and for the highest-pressure points of Grilly and Mills.

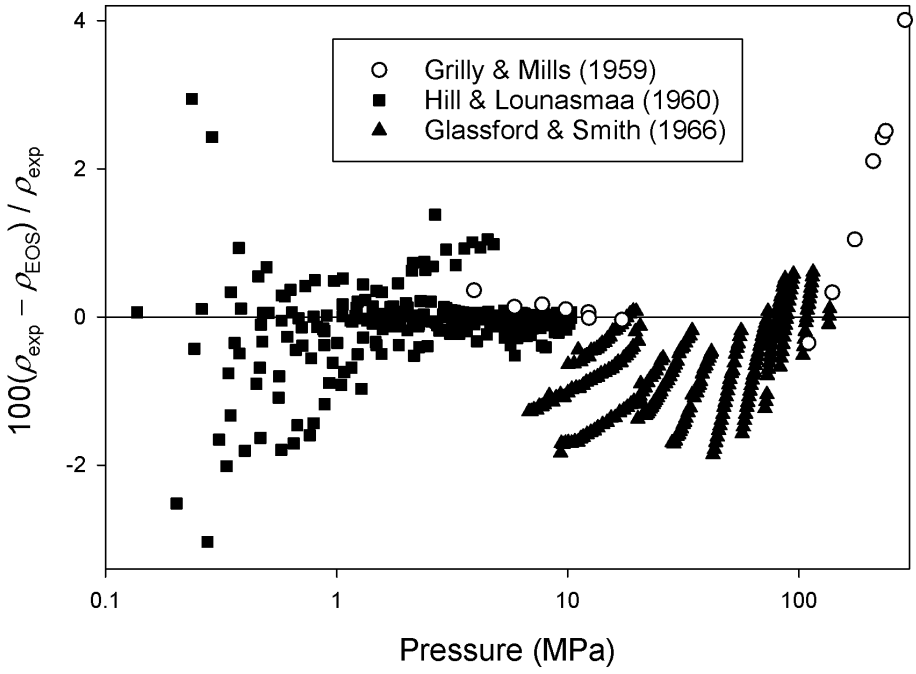

Fig. 9. Relative percent differences between experimental densities [22-24] for compressed liquid and supercritical states (at temperatures up to 30 K) and those calculated with the equation of state. A point at 349 MPa from Ref. [22] with a deviation of +5 % is off the scale of the plot.

5.4. Speed of Sound

The sound speed can provide important information for constraining an equation of state. High-accuracy measurements of the speed of sound in the compressed gas have been reported by Gammon [25] from 98 K to 423 K at pressures from 1 MPa to 15 MPa and by Hurly et al. [26] from 225 K to 400 K at pressures from 0.15 MPa to 1.5 MPa. In the liquid, we compare with the measurements of Van Itterbeek and Forrez [27], Van den Berg et al. [28], and Barmatz and Rudnick [29] for the saturated liquid, and Vignos and Fairbank [30] at saturation and for the compressed liquid up to roughly 5 MPa. Very recently, Wedler and Trusler [31] reported sound speeds in the compressed gas up to 100 MPa from 273 K to 373 K.

Figure 10 shows the gas-phase data. The data of Gammon [25] are described within roughly 0.01 %, except for one isotherm (at 98 K) that displays larger negative deviations. The data of Hurly et al. [26] are somewhat more scattered and systematically high, but still generally reproduced within 0.03 %. We note that data on the y-axis of Fig. 10 should approach zero at low densities, because the ideal-gas behavior is a function only of the molar mass and the molar gas constant, both of which are known.

The new high-pressure gas-phase data of Wedler and Trusler [31], which were not used in fitting the equation of state, have relative expanded uncertainties on the order of 0.03 % and agree with the data of Gammon where they overlap. They show good agreement with the equation of state up to roughly 60 MPa, but above that pressure the equation of state overpredicts the sound speed by amounts that are clearly larger than the uncertainty of the data. This indicates that there is room for improvement of the equation of state for the compressed gas at these high pressures.

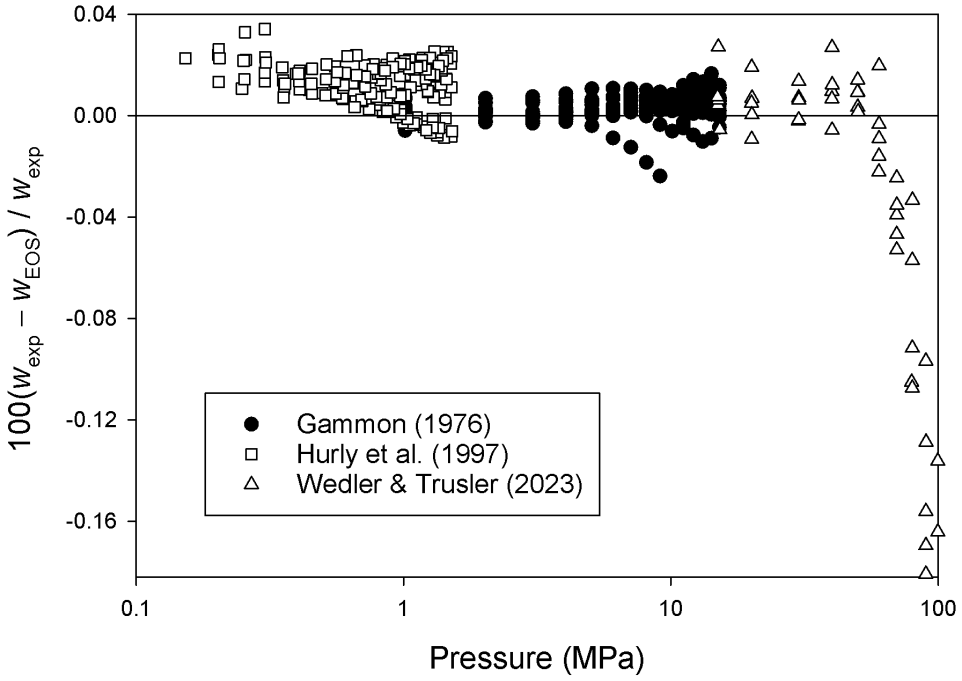

Fig. 10. Relative percent differences between experimental sound speeds [25,26,31] for the gas phase and those calculated with the equation of state. Three points from Ref. [31] near 100 MPa with deviations between –0.2 % and –0.25 % are not shown.

Figure 11 shows the results for liquid sound speeds. The sound speed of the saturated liquid is consistent among all four studies [27-30] and indicates that there is significant room for improvement in the equation of state in this regard, especially around 3 K. The compressed liquid data of Ref. [30] scatter around the equation-of-state results within approximately 2 %. The deviations of the lowest-temperature points of Barmatz and Rudnick [29] change rapidly with temperature because those points are very close to the lambda transition, where the sound speed has a weak anomaly that our equation of state is unable to represent.

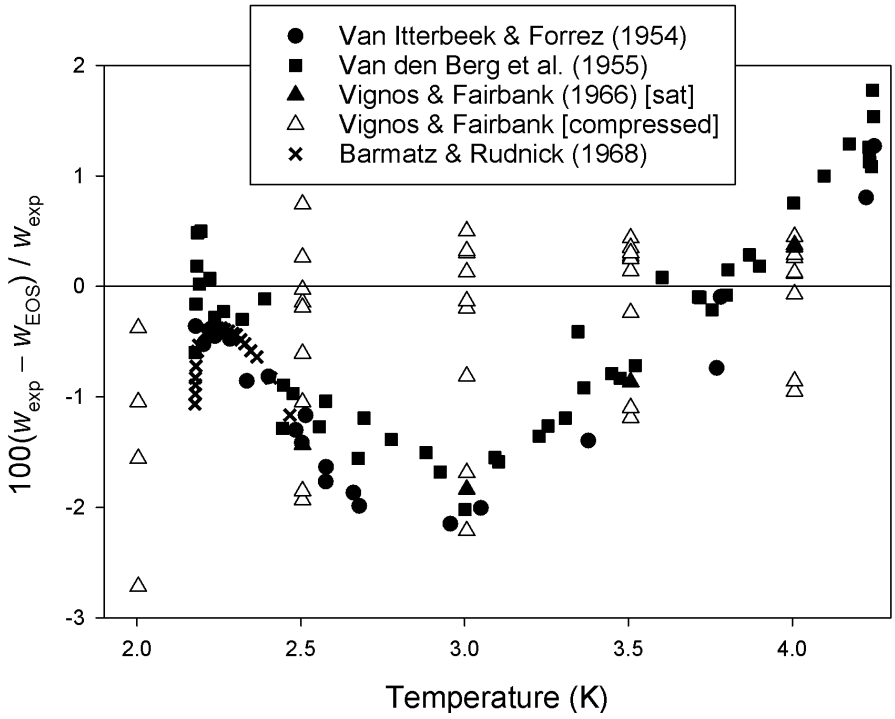

Fig. 11. Relative percent differences between experimental sound speeds [27-30] for the liquid phase and those calculated with the equation of state. All points are for the saturated liquid except for the open triangles from Ref. [30]. Points shown near 2.0 K are those at high enough pressure that they are in the normal (not superfluid) liquid phase.

5.5. Heat Capacity

There have been a number of studies of the heat capacity of helium at cryogenic conditions. Several of those have primarily been concerned with the nonclassical limiting behavior of the isochoric heat capacity c_v near the vapor-liquid critical point or near the lambda transition; we exclude such studies from the present comparison because our classical equation of state cannot quantitatively describe these features.

Hill and Lounasmaa [32] reported smoothed values of the saturated heat capacity c_{sat} along the vapor-pressure curve up to 5.06 K, along with seven of their raw data points. The claimed accuracy was 1 %. The isochoric heat capacity c_v was reported by Lounasmaa and Kojo [33] at temperatures below 3 K and by Hill and Lounasmaa [23] up to 20 K; the pressures in these studies remained below 10 MPa. Dugdale and Franck [34] reported smoothed values of c_v from 7 K up to 29 K at higher densities corresponding in some cases to pressures near 200 MPa.

Figure 12 shows the results for c_{sat}. Most of the experimental data are reproduced within 2%, but many of them are outside the claimed experimental accuracy of 1 %. The deviations in c_{sat} near 3 K look similar to those in the sound speed for the saturated liquid shown in Fig. 11.

Figure 13 shows some of the deviations for c_v as a function of temperature. Not visible on the plot are the two highest-density isochores of Dugdale and Franck [34], which lie mostly above 20 K and show relative deviations on the order of −15 %; the pressures for these points are all above 50 MPa. A number of low-temperature points from Lounasmaa and Kojo [33] have deviations that are off the scale of Fig. 13; these deviations occur within roughly 0.3 K of the

lambda curve. A few of the points from Hill and Lounasmaa [23] that are near the critical point also have larger deviations. The remaining points are reproduced within approximately 3 %.

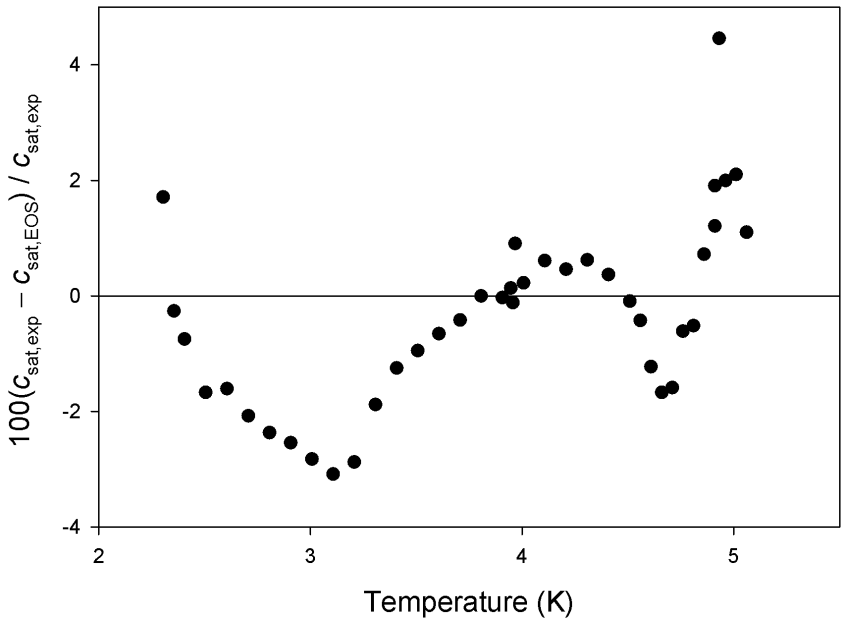

Fig. 12. Relative percent differences between experimental c_{sat} [32] and those calculated with the equation of state.

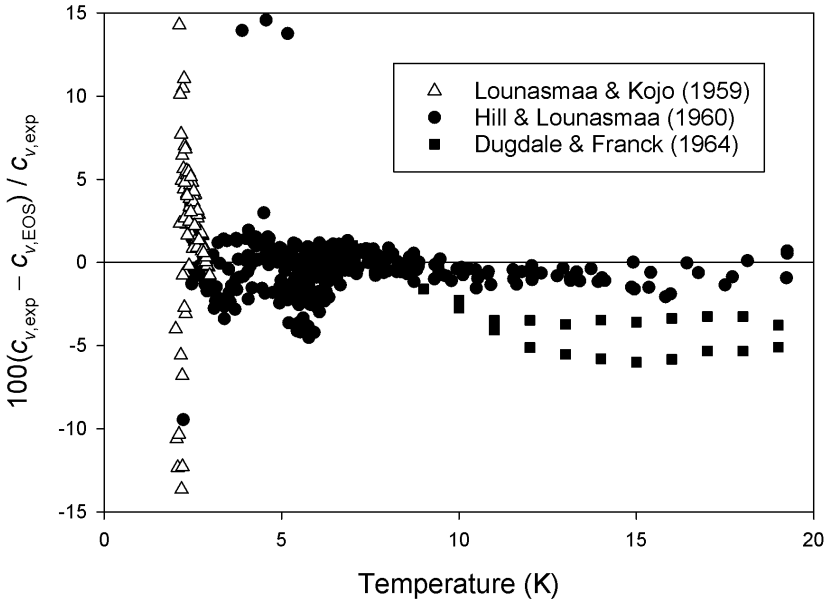

Fig. 13. Relative percent differences between experimental isochoric heat capacities [23,33,34] and those calculated with the equation of state.

6. Comments Concerning Uncertainty

Because of the issues mentioned in Sec. 1, we refrain from making definitive uncertainty claims for this preliminary equation of state. The figures in Sec. 5 indicate the level of agreement with experimental data, which is related to the uncertainty. The vapor-pressure deviations in Fig. 1 show the error in that quantity. Vapor densities are accurate to 0.02 % or better at least up to 40 MPa (Figs. 6 and 7). The saturated liquid density is described within 0.2 % for most of the temperature range, with higher deviations as the critical point is approached (Fig. 8). Compressed liquid densities are described to within 2 % up to 100 MPa (Fig. 9). The sound speed of the compressed vapor is accurate to within 0.02 % up to roughly 60 MPa, with larger deviations at higher pressures (Fig. 10). Liquid-phase sound speeds exhibit larger deviations, on the order of 2 % (Fig. 11). Heat capacities for the liquid and for the dense supercritical fluid at cryogenic temperatures have deviations on the order of 3 % (Figs. 12 and 13).

Uncertainties are higher near the critical point (where our classical equation of state cannot quantitatively reproduce the critical phenomena) and near the λ curve. Some effort was made during the fitting process to mimic the qualitative behavior of properties such as c_v near the λ curve, but, as shown in Fig. 13, quantitative accuracy is lacking.

7. Range of Validity

The equation of state is valid for the normal fluid (helium I) from the low-pressure endpoint of the λ curve on the vapor-liquid saturation boundary (2.1768 K) to 1500 K for pressures up to 2000 MPa. It extrapolates in a physically reasonable manner to lower temperatures at higher pressures within the helium I phase in the region bounded by the λ curve that extends to its intersection with the melting curve at roughly 1.76 K and 3.0 MPa. It is not valid for the superfluid (helium II) region or in the asymptotic limit as the λ curve is approached. The range of validity is also bounded at low temperatures by the melting curve, which we take from the work of McCarty and Arp [7].

8. Check Values

For purposes of checking computer implementations, Table 3 gives values of several properties computed in the single-phase region at the specified temperatures and densities. Table 4 contains the vapor pressure p_{sat} as well as properties of the saturated liquid (density ρ', enthalpy h') and saturated vapor (density ρ'', enthalpy h'') at temperatures from 2.2 K (just above the lambda transition) to 5.15 K (just below the critical temperature). The methods for calculating properties from a Helmholtz energy equation of state have been described elsewhere [35,36].

The large number of digits given in Tables 3 and 4 is merely for the purpose of verifying that calculations with the equation of state have been implemented correctly; the number of digits is not indicative of the uncertainty of the equation of state, which is discussed in Sec. 6.

Table 3. Calculated thermodynamic properties in the single-phase region at selected values of temperature T and molar density ρ.

T (K)	ρ (mol dm^{-3})	p (MPa)	c_v (J mol^{-1} K^{-1})	Sound speed (m s^{-1})
4	40.0	1.593262	8.098737	320.1490
4	2.0	0.0554523	12.627957	107.3812
10	50.0	12.65519	10.753076	592.9440
10	2.0	0.1588571	12.478387	183.7793
300	25.0	85.769640	13.176055	1349.3067
300	1.0	2.524130	12.496256	1030.3609

Table 4. Calculated thermodynamic properties at vapor–liquid saturation.

T (K)	p_{sat} (kPa)	ρ' (mol dm^{-3})	ρ'' (mol dm^{-3})	h' (J mol^{-1})	h'' (J mol^{-1})
2.2	5.3317	36.474	0.30776	–27.1597	63.8799
2.4	8.3507	36.321	0.45005	–24.9634	67.0948
2.6	12.376	36.050	0.62860	–22.9856	70.0799
2.8	17.562	35.697	0.84784	–20.9686	72.8144
3.0	24.061	35.277	1.1127	–18.8099	75.2766
3.2	32.024	34.796	1.4288	–16.4582	77.4416
3.4	41.599	34.251	1.8032	–13.8784	79.2798
3.6	52.936	33.638	2.2451	–11.0375	80.7528
3.8	66.186	32.947	2.7666	–7.8975	81.8099
4.0	81.509	32.164	3.3847	–4.4081	82.3803
4.2	99.076	31.264	4.1250	–0.4980	82.3597
4.4	119.076	30.209	5.0278	3.9418	81.5857
4.6	141.732	28.931	6.1636	9.0949	79.7820
4.8	167.324	27.296	7.6731	15.3181	76.4226
5.0	196.235	24.944	9.9203	23.5348	70.1954
5.1	212.110	23.109	11.705	29.4075	64.6840
5.15	220.461	21.690	13.102	33.6962	60.1771

References

[1] Ortiz Vega DO (2013) A New Wide Range Equation of State for Helium-4. Ph.D. Thesis. (Texas A&M University, College Station).

[2] Lemmon EW, Bell IH, Huber ML, McLinden MO (2018) NIST Standard Reference Database 23: Reference Fluid Thermodynamic and Transport Properties-REFPROP, Version 10.0 (National Institute of Standards and Technology, Standard Reference Data Program, Gaithersburg). https://doi.org/10.6028/T4/1502528

[3] Preston-Thomas H (1990) The International Temperature Scale of 1990 (ITS-90). *Metrologia* 27:3. https://doi.org/10.1088/0026-1394/27/1/002

[4] Harvey AH (2021) What the thermophysical property community should know about temperature scales. *International Journal of Thermophysics* 42:165. https://doi.org/10.1007/s10765-021-02915-9

[5] Puchalski M, Szalewicz K, Lesiuk M, Jeziorski B (2020) QED calculation of the dipole polarizability of helium atom. *Physical Review A* 101:022505. https://doi.org/10.1103/PhysRevA.101.022505
[6] Garberoglio G, Gaiser C, Gavioso RM, Harvey AH, Hellmann R, Jeziorski B, Meier K, Moldover MR, Pitre L, Szalewicz K, Underwood R (2023) Ab initio calculation of fluid properties for precision metrology. *Journal of Physical and Chemical Reference Data*, in press. https://doi.org/10.1063/5.0156293
[7] McCarty RD, Arp, VD (1990) A new wide range equation of state for helium. *Advances in Cryogenic Engineering* 35:1465. https://doi.org/10.1007/978-1-4613-0639-9_174
[8] Tiesinga E, Mohr PJ, Newell DB, Taylor BN (2021) CODATA recommended values of the fundamental physical constants: 2018. *Journal of Physical and Chemical Reference Data* 50:033105. https://doi.org/10.1063/5.0064853
[9] Mehl JB (2009) Ab initio properties of gaseous helium. *Comptes Rendus Physique* 10:859. https://doi.org/10.1016/j.crhy.2009.10.009
[10] Garberoglio G, Moldover MR, Harvey AH (2011) Improved first-principles calculation of the third virial coefficient of helium. *Journal of Research of the National Institute of Standards and Technology* 116:729. https://doi.org/10.6028/jres.125.019
[11] Czachorowski P, Przybytek M, Lesiuk M, Puchalski M, Jeziorski B (2020) Second virial coefficients for ^{4}He and ^{3}He from an accurate relativistic interaction potential. *Physical Review A* 102:042810. https://doi.org/10.1103/PhysRevA.102.042810
[12] Binosi D, Garberoglio G, Harvey AH (2023) The third density and acoustic virial coefficients of helium isotopologues from *ab initio* calculations. *Journal of Chemical Physics*, in preparation.
[13] McLinden MO, Lösch-Will C (2007) Apparatus for wide-ranging, high-accuracy fluid (p,ρ,T) measurements based on a compact two-sinker densimeter. *Journal of Chemical Thermodynamics* 39:507. https://doi.org/10.1016/j.jct.2006.09.012
[14] Blancett AL, Hall KR, Canfield FB (1970) Isotherms for the He-Ar system at 50°C, 0°C and –50°C up to 700 atm. *Physica* 47:75. https://doi.org/10.1016/0031-8914(70)90101-1
[15] Garberoglio G, Harvey AH (2021) Path-integral calculation of the fourth virial coefficient of helium isotopes. *Journal of Chemical Physics* 154:104107. https://doi.org/10.1063/5.0043446
[16] Schultz AJ, Kofke DA (2019) Virial coefficients of helium-4 from *ab initio*-based molecular models. *Journal of Chemical & Engineering Data* 64:3742. https://doi.org/10.1021/acs.jced.9b00183
[17] Moldover MR, McLinden MO (2010) Using *ab initio* "data" to accurately determine the fourth density virial coefficient of helium. *Journal of Chemical Thermodynamics* 42:1193. https://doi.org/10.1016/j.jct.2010.02.015
[18] Garberoglio G, Harvey AH (2020) Path-integral calculation of the second dielectric and refractivity virial coefficients of helium, neon, and argon. *Journal of Research of the National Institute of Standards and Technology* 125:125022. https://doi.org/10.6028/jres.125.022
[19] Kerr EC (1957) Density of liquid He^4. *Journal of Chemical Physics* 26:511. https://doi.org/10.1063/1.1743334
[20] Kerr EC, Taylor RD (1964) The molar volume and expansion coefficient of liquid He^4. *Annals of Physics* 26:292. https://doi.org/10.1016/0003-4916(64)90158-7

[21] El Hadi ZEHA, Durieux M, van Dijk H (1969) The density of liquid ^{4}He under its saturated vapour pressure. *Physica* 41:289. https://doi.org/10.1016/0031-8914(69)90119-0
[22] Grilly ER, Mills RL (1959) Melting properties of He^3 and He^4 up to 3500 kg/cm^2. *Annals of Physics* 8:1. https://doi.org/10.1016/0003-4916(59)90061-2
[23] Hill RW, Lounasmaa OV (1960) The thermodynamic properties of fluid helium. *Philosophical Transactions of the Royal Society of London, Series A* 252:357. https://doi.org/10.1098/rsta.1960.0009
[24] Glassford APM, Smith JL (1966) Pressure-volume-temperature and internal energy data for helium from 4.2 to 20 K between 100 and 1300 atm. *Cryogenics* 6:193. https://doi.org/10.1016/0011-2275(66)90068-3
[25] Gammon BE (1976) The velocity of sound with derived state properties in helium at −175 to 150 °C with pressure to 150 atm. *Journal of Chemical Physics* 64:2556. https://doi.org/10.1063/1.432508
[26] Hurly JJ, Schmidt JW, Boyes SJ, Moldover MR (1997) Virial equation of state of helium, xenon, and helium-xenon mixtures from speed-of-sound and Burnett $P\rho T$ measurements. *International Journal of Thermophysics* 18:579. https://doi.org/10.1007/BF02575125
[27] Van Itterbeek A, Forrez G (1954) First sound measurements in liquid helium. *Physica* 20:133. https://doi.org/10.1016/S0031-8914(54)80025-5
[28] Van den Berg GJ, Van Itterbeek A, Van Aardenne GMV, Herfkens, JHJ (1955) Determination of the velocity of ultrasonic waves in liquid helium by the optical method. *Physica* 21:860. https://doi.org/10.1016/S0031-8914(55)92478-2
[29] Barmatz M, Rudnick I (1968) Velocity and attenuation of first sound near the λ point of helium. *Physical Review* 170:224. https://doi.org/10.1103/PhysRev.170.224
[30] Vignos JH, Fairbank HA (1966) Sound measurements in liquid and solid He^3, He^4, and He^3-He^4 mixtures. *Physical Review* 147:185. https://doi.org/10.1103/PhysRev.147.185
[31] Wedler C, Trusler JPM (2023) Speed of sound measurements in helium at pressures from 15 to 100 MPa and temperatures from 273 to 373 K. *Journal of Chemical & Engineering Data* 68:1305. https://doi.org/10.1021/acs.jced.3c00083
[32] Hill RW, Lounasmaa OV (1957) The specific heat of liquid helium. *Philosophical Magazine* 2:143. https://doi.org/10.1080/14786435708243803
[33] Lounasmaa OV, Kojo E (1959) The specific heat C_v of liquid helium near the λ-curve at various densities. *Annales Academiæ Scientiarum Fennicæ, Series A. VI. Physica* 36:1.
[34] Dugdale JS, Franck JP (1964) The thermodynamic properties of solid and fluid helium-3 and helium-4 above 3 °K at high densities. *Philosophical Transactions of the Royal Society A* 257:1. https://doi.org/10.1098/rsta.1964.0012
[35] Span R (2000) *Multiparameter Equations of State: An Accurate Source of Thermodynamic Property Data* (Springer, Berlin).
[36] Lemmon EW, Jacobsen RT (2005) A new functional form and new fitting techniques for equations of state with application to pentafluoroethane (HFC-125). *Journal of Physical and Chemical Reference Data* 34:69. https://doi.org/10.1063/1.1797813